MARTIN MARIETTA ENERGY SYSTEMS LIBRARIES
3 4456 0149061 9

ORNL/TM-9998

ornl

OAK RIDGE NATIONAL LABORATORY

MARTIN MARIETTA

Viscosity Behavior in Supercooled Pure Liquids and Mixtures

J. A. Hughes
C. H. Byers

OAK RIDGE NATIONAL LABORATORY
CENTRAL RESEARCH LIBRARY
CIRCULATION SECTION
4500N ROOM 175
LIBRARY LOAN COPY
DO NOT TRANSFER TO ANOTHER PERSON
If you wish someone else to see this report, send in name with report and the library will arrange a loan.

OPERATED BY
MARTIN MARIETTA ENERGY SYSTEMS, INC.
FOR THE UNITED STATES
DEPARTMENT OF ENERGY

Printed in the United States of America. Available from
National Technical Information Service
U.S. Department of Commerce
5285 Port Royal Road, Springfield, Virginia 22161
NTIS price codes—Printed Copy: A04; Microfiche A01

This report was prepared as an account of work sponsored by an agency of the United States Government. Neither the United States Government nor any agency thereof, nor any of their employees, makes any warranty, express or implied, or assumes any legal liability or responsibility for the accuracy, completeness, or usefulness of any information, apparatus, product, or process disclosed, or represents that its use would not infringe privately owned rights. Reference herein to any specific commercial product, process, or service by trade name, trademark, manufacturer, or otherwise, does not necessarily constitute or imply its endorsement, recommendation, or favoring by the United States Government or any agency thereof. The views and opinions of authors expressed herein do not necessarily state or reflect those of the United States Government or any agency thereof.

ORNL/TM-9998

Chemical Technology Division

VISCOSITY BEHAVIOR IN SUPERCOOLED PURE LIQUIDS AND MIXTURES

J. A. Hughes*
C. H. Byers

*Department of Mechanical Engineering, Duke University, Durham, North Carolina 27706.

Date of Issue - December 1986

Prepared by the
OAK RIDGE NATIONAL LABORATORY
Oak Ridge, Tennessee 37831
operated by
MARTIN MARIETTA ENERGY SYSTEMS, INC.
for the
U.S. DEPARTMENT OF ENERGY
under Contract No. DE-AC05-84OR21400

MARTIN MARIETTA ENERGY SYSTEMS LIBRARIES
3 4456 0149061 9

CONTENTS

ABSTRACT vii

1. INTRODUCTION 1

2. THEORETICAL BACKGROUND 2

3. EXPERIMENTAL METHODS AND MATERIALS 6

3.1 CAPILLARY VISCOMETRY 6

3.2 LASER LIGHT-SCATTERING METHOD 10

3.3 MATERIALS 14

4. EXPERIMENTAL RESULTS 15

4.1 PHENOL VISCOSITY 16

4.2 TERTIARY BUTANOL DATA 22

4.3 VISCOSITY TIME DEPENDENCE 31

4.4 LASER LIGHT-SCATTERING STUDIES 35

5. DISCUSSION 36

6. CONCLUSIONS 40

7. RECOMMENDATIONS 41

8. REFERENCES 42

APPENDIX A 47

APPENDIX B 51

LIST OF FIGURES

ORNL DWG NO.	CAPTION	PAGE
84-576R2	Fig. 1. Capillary viscometer apparatus for fluids in the temperature range 273 to 400 K	8
85-17560	Fig. 2. Dynamic light-scattering spectrometer with auxiliary equipment for the measurement of viscosities in the subcritical region	13
85-1104R	Fig. 3. Viscosity of phenol in the region of the melting point. Lines indicate the Andrade correlation fitting of the data in the two regions	17
85-17566	Fig. 4. Phenol viscosity data deviations from the Andrade correlation for above-melting point-data ..	18
86-823	Fig. 5. Antoine relationship for pure phenol [(A = -1.366) (B = 269.48 K) (Tg = -181 K) (xx data — correlation)]	21
85-17568	Fig. 6. Viscosity of pure t-butanol in the region of the melting point. Lines indicate the Andrade correlation fitting of the data in the two regions.	23
85-17567	Fig. 7. Pure t-butanol viscosity data deviations from the Andrade correlation for above-melting-point data	24
86-821	Fig. 8. Antoine relationship for pure t-butanol [(A = -4.06922 mPa•s) (B = 920 K) (Tg = -103 K) (xx Data — correlation)]	26
85-17564	Fig. 9. Viscosity of pure t-butanol containing 0.06 wt % ethanol in the region of the mixture melting point. Lines indicate the Andrade correlation fitting of the data above and below the pure t-butanol melting point	27
85-17569	Fig. 10. Viscosity of pure t-butanol containing 0.6 wt % ethanol in the region of the mixture melting point. Lines indicate the Andrade correlation fitting of the data above and below the pure t-butanol melting point	28
85-17565	Fig. 11. Viscosity of pure t-butanol containing 1.0 wt % ethanol in the region of the mixture melting point. Lines indicate the Andrade correlation fitting of the data above and below the pure t-butanol melting point	29

86-822 Fig. 12. Antoine relation for t-butanol containing 1% ethanol [(x data) (— correlation all data) (— — — high-temperature correlation) (---- low-temperature correlation)] 32

85-17572 Fig. 13. Viscosity functionality in time for the t-butanol -0.06% ethanol system above and below the normal boiling point (■ - below freezing; ●●● - above freezing) 33

85-17573 Fig. 14. Viscosity functionality in time for pure phenol above and below the normal boiling point (■ - below freezing point; ● - above freezing point) 34

VISCOSITY BEHAVIOR IN SUPERCOOLED PURE LIQUIDS AND MIXTURES

J. A. Hughes* and C. H. Byers

ABSTRACT

Under relatively quiescent conditions, it is often possible to maintain fluids in a liquid state at temperatures below their freezing point. Viscosities of phenol and t-butanol in the freezing-point region deviate significantly from the Andrade correlation. Two Andrade curves, one above and one below the freezing point, cross at approximately the freezing point and fit the data well. An Antoine-type relationship fits all the phenol data well, but two such curves are required to fit the t-butanol data. The activation energy term in the Andrade equation increases significantly when the temperature drops below the freezing point. This may be interpreted as being the result of cluster formation in the liquid, or at least the establishment of more short-range order in the supercooled fluid. Mixtures containing up to 1 mol % ethanol in t-butanol behaved, from a viscosity viewpoint, in a manner similar to pure t-butanol, that is, the viscosity relationship changed at the freezing point of the pure fluid and not at the freezing point of the mixture.

The time dependence of the supercooled viscosity of the pure fluids was explored. Repeated experiments indicate that the viscosity of a supercooled fluid slowly decreases with time, with the total variation of ~0.05 Pa.s/d. This phenomenon does not occur above the melting point of these same fluids. It is possible that this is a manifestation of molecular or cluster rearrangements. Broader confirmation of this phenomenon is required.

1. INTRODUCTION

Methods of predicting the behavior of materials are very important to the successful design and operation of many engineering systems. Of the three states of matter, solids, liquids, and gases, liquids have traditionally been the most difficult to model and, therefore, for which to develop accurate prediction methods. Even less information is available concerning liquids existing in a metastable supercooled state below their natural melting point.

Gathering and examining information about liquids in the supercooled state will not only provide valuable insights into the nature of supercooled liquids but will also add to our knowledge of liquids in general. As viscosity is an important property of any liquid, viscosity information is necessary in the designing of various pumps and piping systems as well as for predicting the performance of various types of separation equipment. From a fundamental viewpoint, viscosity is a direct indication of intermolecular potential, as it is a dynamic molecular property dependent on the molecular size and structure. This dependence on molecular structure, combined with its engineering importance, makes viscosity an appropriate tool for examining the phenomenon of supercooling and any resulting structural changes.

There is a significant amount of data from past experiments with supercooled liquids indicating deviations, discontinuities, and abnormalities in the properties of liquids as they pass through the melting point into the supercooled region.[1-4] Our study has begun to gather more information on the relationship of supercooling to fluid forces and structure. Special emphasis is to be placed on reproducing past experiments and analyzing the effects of time and chemical purity. It

is hoped that this investigation will lead to new insights concerning the forces and clustering in liquids and the structure of supercooled liquids in particular.

2. THEORETICAL BACKGROUND

Our ability to predict transport properties of a medium depends heavily upon our understanding of the intermolecular potential and spacing characteristics of the fluid. As the liquid phase is the least well described and by far the most complex of the three phases of matter, it is perhaps natural to use extensions of gas and solid state theory to fill the middle ground. Indeed, that is the thrust of the vast majority of the modeling work in dense gas theory and lattice theory of liquids. These theories lead to intermolecular potentials, which allow a prediction of viscosity and diffusion coefficient from first principles. Unfortunately, these are poor approximations of measured properties, with the exception of the region near the critical point.

One would expect the structure and force fields of supercooled liquids to be very similar to those of the liquid above its melting point. Past studies[1-6] have shown the behavior of such fluids to be anomalous in a number of cases. A study of some hydrogen-bonded systems in which anomalies have been noted is of particular interest in learning more about cryonucleation and crystallization from melts.

The basic theory of viscosity and fluid motion has been reviewed in a number of texts.[7-9] As we pointed out earlier, these theories are more indicative of trends that are serving as predictive tools. In fact, the empirical and semiempirical approaches to the prediction have far greater

utility for predictive purposes than the fundamentally derived empirical methods.

A number of empirical and semiempirical methods have been developed in an effort to predict the viscosities of pure liquids in a restricted temperature range above their melting points. The Orrick and Ebar method uses a group contribution technique to estimate A and B in the following equation:[9]

$$\ln\frac{\mu_L}{\rho_L M} = A + \frac{B}{t}, \tag{1}$$

where ρ_L is the liquid density at 20°C.

Thomas suggests a similar empirical method:[9]

$$\log\left[8.509\ \frac{\mu_L}{\rho_L}\right] = \phi\left(\frac{1}{Tr} - 1\right), \tag{2}$$

where

Tr = reduced temperature, T/Tc,

ϕ = viscosity constant.

Another commonly cited method is in the form of the Morris equation:[9]

$$\log\left[\frac{\mu_L}{\eta}\right] = J\left(\frac{1}{Tr} - 1\right). \tag{3}$$

The method of Van Velzen, Cardozo, and Langenkamp[9] deserves special attention due to the dependence of its extra-heavy group contribution on the structure of the liquid.

$$\log \left[\mu_L\right] = B\left(\frac{1}{T} - \frac{1}{T_o}\right), \tag{4}$$

with B and T_o determined from the liquid's particular structure.

These methods have large errors, with average errors ranging from 15 to 20% and individual errors occurring as high as 100%. Close examination of the viscosity-structure relationship assumptions of the various methods along with their actual errors in predicting viscosity can lead to valuable insights into the actual viscosity-structure relationship. Some attempts should be made to apply these methods to supercooled liquids — something which has not been done as yet.

As more data are accumulated on supercooled liquid properties, it is possible that these methods will be improved. Many of the constants in these methods, as well as experimental correlations, are often fitted to other physical properties, such as vapor pressure, latent heat of vaporization, and bond strengths. The validity of these assumed relationships will be tested by comparing the changes in viscosity during supercooling with the changes in other properties during supercooling.

If any experimental viscosity data are available for a particular liquid, the empirical prediction methods are avoided in favor of an experimental correlation known as the Andrade correlation:

$$\mu_L = Ae^{B/T}, \tag{5}$$

where A and B are experimentally fitted constants. Although many slightly more complicated correlations have been suggested, the Andrade correlation is still the most widely used and was applied with good results in this

study. The two constants, A and B, are the frequency factor and the activation energy, respectively, in an Arrhenius-type expression. Most of the previously mentioned relationships are attempts to present means of predicting the two constants.

Another relationship, suggested by Fulcher[10] and Tammann and Hesse,[11] takes on the Antoine equation form:

$$\ln \mu = A' + \frac{B'}{T - T_o} . \tag{6}$$

This is, of course, a three-constant equation, and as a result, would be expected to fit over a wider range of temperatures. It postulates an activation energy of the form:

$$E = E_o/(a + b/T) . \tag{7}$$

This last relationship is difficult to justify based upon normal thermodynamic concepts. On the other hand, it has been shown by such workers as Dolittle and Dolittle[12] and Cohen and Turnbull[13] that

$$\ln n = A + B(v_o/v_f) ,$$

where v_o is the specific volume of the fluid at absolute zero. Over a wide temperature range, the specific volume varies linearly with temperature; therefore, the Antoine-type relationship has some theoretical basis.

A third, widely used empirical form of the viscosity-temperature relationship is

$$\ln n = A + B/T^n . \tag{8}$$

Litovitz[14] found that a value for n of 3 represents associated fluids over a range of ~100°C above and below the normal melting point. A value of 4 was espoused by Barlow and Lamb[15] to fit the viscosity of lubricating oils over a 40°C range. It has been found to be a useful fitting equation, but its theoretical soundness is questionable.

3. EXPERIMENTAL METHODS AND MATERIALS

3.1 CAPILLARY VISCOMETRY

The relative merits of the various methods of measuring viscosity have been reviewed by Van Wazer.[16] Among the simplest and most accurate means is the use of a capillary viscometer with which the flow rate through a circular tube of fixed length is measured using a fluid of known density. The Hagen-Poiseuille equation, which is the solution of the Navier-Stokes equations for laminar flow through a circular tube, is then used to calculate viscosity of the unknown fluid. Thus,

$$\mu = \frac{\pi}{8}\left(\frac{\Delta P \cdot R^4}{L \cdot \Delta V}\right)\Delta t \ , \tag{9}$$

where

Δt = efflux time,

ΔV = efflux volume,

ΔP = average hydrostatic head = $\rho \cdot \bar{z}$,

R = average capillary radius,

L = capillary length.

Implicit in this solution are assumptions of steady laminar flow, a Newtonian medium, incompressibility, and a nonslip wall condition. In

a capillary viscometer, nonideal conditions, such as variations in radius, capillarity effects, entrance and exit flow irregularities, and kinetic energy contributions, make it mandatory that corrections be made to the Hagen-Poiseuille equation.[8] These corrections are tedious to predict and contribute inaccuracies; therefore, it is usual to calibrate the viscometer with a fluid of known viscosity.

Equation (9) may be rearranged as follows:

$$\nu = \mu/\rho = K_{uc}\,\Delta t - KE_{uc}/\Delta t^2 \ , \tag{10}$$

where the calibration constant, Kl_{uc}, is

$$Kl_{uc} = \frac{\pi}{4}\left(\frac{z \cdot R^4}{L \cdot \Delta V}\right),$$

and KE_{uc} equals kinetic energy correction constant. The geometry of the particular viscometer determines the average radius, R, effective length, L, and the volume of the draining reservoir, V. This allows the calculation of K_{uc} based on the observed time required to drain the reservoir. Over a moderate temperature range, K_{uc} will remain constant. For the systems examined in the current study, water is an excellent calibration fluid.

The major component of the apparatus used in this study, as shown schematically in Fig. 1, is a glass Ubbelohde viscometer manufactured by Schott Gerate (Model Series 24500). Normal viscometer operation involves drawing the sample fluid into a reservoir bulb and measuring the time required for the gravity efflux of a fluid volume defined by etched lines

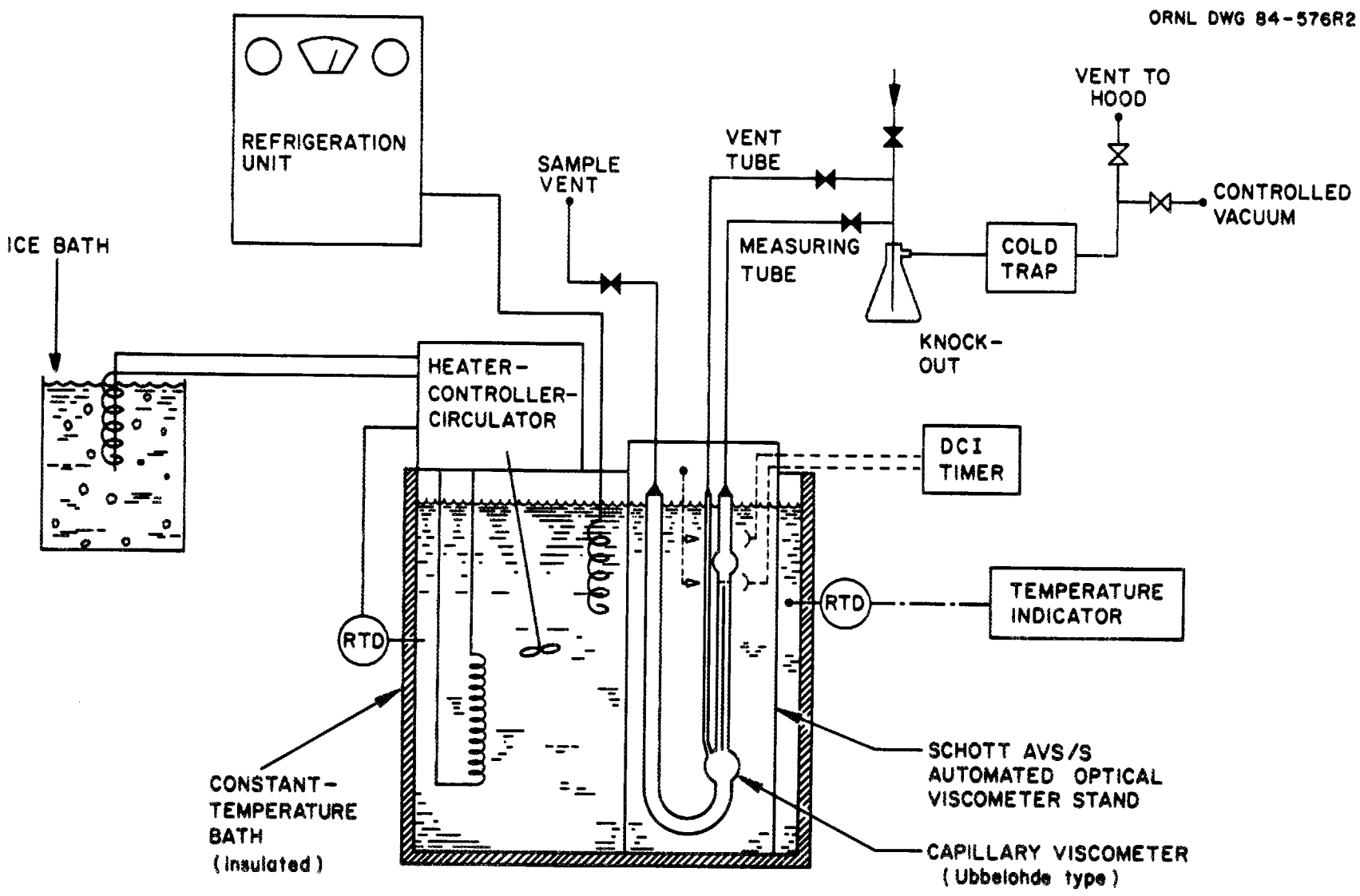

Fig. 1. Capillary viscometer apparatus for fluids in the temperature range 273 to 400 K.

above and below the bulb. This process is automated in the Schott viscometer, and fiber-optic detectors replace the etched volume lines. When the fluid interface passes the plane of a light beam from the transmitter to a detector unit, the voltage signal changes, starting a timer. As the interface passes a second detector, denoting the flux of a fixed volume, the signal change stops the electronic timer. Efflux time can be determined accurately to within 0.01 s, essentially removing one of the persistent sources of experimental error in older devices. More details on the operation of capillary viscometers may be found in the literature.[17-19]

The experimental equipment also included a constant-temperature bath and a piping system for drawing samples into the capillary tube. Because temperatures below that of process water were often required, a cooling system was attached to the bath. To ensure rapid removal of heat, a piping system was attached to a coiled heat exchanger which could alternately be immersed in ice water or room-temperature water, depending on whether heating or cooling was desired. To maintain cooler temperatures, a Freon fluid refrigerator coil was used within the bath. The temperature bath was a Maake, Model N2, recirculating unit placed in a well-insulated cylindrical glass bath. Measurements were made at temperatures between 17 and 70°C with control to within 0.02°C. The distilled water, which was used at all times as the bath medium, was initially heated and held at 100°C for a short time to pass off as many oxygen bubbles as possible to prevent bubbles from lodging in the light path and triggering the timing device during runs. A calibrated platinum resistance thermometer connected to a digital Fluke RTD sensor (Model #2180A) made it possible to measure temperatures accurately to within 0.1°C. The entire unit

(except readout devices) was covered and heavily insulated to minimize temperature gradients.

Viscometers were kept rigorously clean throughout the experimental period by first rinsing them in a 3 M solution of potassium hydroxide in ethanol, followed by washing in acetone and water, and overnight soaking in chromic acid. Sonication was often used, followed by a water rinse, an acetone wash, and purified air drying.

Readings were made on liquids kept within the viscometer for a period of 10 min to 24 h. When experiments were not in progress, air flow to the sample was restricted by metal clamps over all the tubing systems, thus isolating the test fluid.

The viscometer stand, on which the fiber-optic detectors are precisely affixed, allows the rapid interchange of viscometers. During the course of the study, several glass units were used. In all instances, the manufacturer (Schott Gerate) provided calibration constants, K_{uc} and KE_{uc}, which relate the efflux time, t, to the kinematic viscosity, ν, as in Eq. (10). To obtain the dynamic viscosity, μ, it is necessary to determine the density of the fluid at the temperature of the experiment (see Appendix A).

3.2 LASER LIGHT SCATTERING METHOD

The use of dynamic laser light scattering, a relatively new method of measuring a liquid's viscosity, was attempted in this study. The procedure for measuring viscosity using light scattering is based on the principle that laser light focused through a liquid sample will result in light scattering if dielectric fluctuations (heterogeneities) exist in the liquid. It is important to note that a perfectly homogeneous

medium is incapable of scattering light, and no net scattering will be observed in such a medium. It is possible to relate the scattered light signal from a heterogeneous medium to the physical properties governing the medium, therefore measuring those properties such as viscosity and particle diameter.

Monodisperse colloidal particles in a fluid suspension exhibit Brownian motion. Brownian motion of particles in a fluid is promoted by collisions with molecules of the fluid and retarded by the effect of the fluid's viscous drag. The scattered-light intensity undergoes a Doppler shift in intensity due to the motion of the free particles. The Brownian motion of these particles can be described by the Langevin equation:[20]

$$\frac{d\bar{u}}{dt} = -\beta\ u + \bar{A}(t)\ , \tag{11}$$

where

$\bar{u}$ = particle velocity vector,

t = time,

β = coefficient of dynamic friction,

$\bar{A}(t)$ = fluctuating influence of molecular collision process characteristic of molecular Brownian motion.

For a spherical particle, the coefficient of dynamic friction is given by Stokes' law:

$$\beta = 6\pi a\eta/m\ , \tag{12}$$

where

a = particle radius,

η = fluid viscosity,

m = particle mass.

The diffusion coefficient, D, is another important term in relating the light-scattering shift to the actual properties of a liquid. The Stokes-Einstein relation defines D as:

$$D = \frac{K_b T}{6\pi\eta r} , \tag{13}$$

where

K_b = Boltzmann's constant,

T = temperature,

η = fluid viscosity ,

r = particle radius.

If the viscosity of a substance is known, the diameter of the suspended particles within that substance can be calculated using correlation functions and the diffusion coefficient. In a similar manner, if the diameter of seed particles is known, correlations of Doppler shift-induced light-intensity fluctuations will provide the liquid's viscosity. The absence of particles or the polydispersity of particles makes this method impossible. Further discussion of this technique may be found in Williams.[20]

The equipment used in this study consisted of a 2-W argon ion laser optics detector and signal processing equipment (Fig. 2). The laser generates a vertically polarized beam ($\alpha = \beta$) that is focused to a narrow width and passed through a square cell which contains the sample fluid. The scattered light is collected at a 90° angle to the incident light in a photomultiplier tube, which, in turn, is conditioned in pulse amplifier-discrimination. An auto correlator (Langley Ford model 1096) is used to

ORNL DWG 85-17570

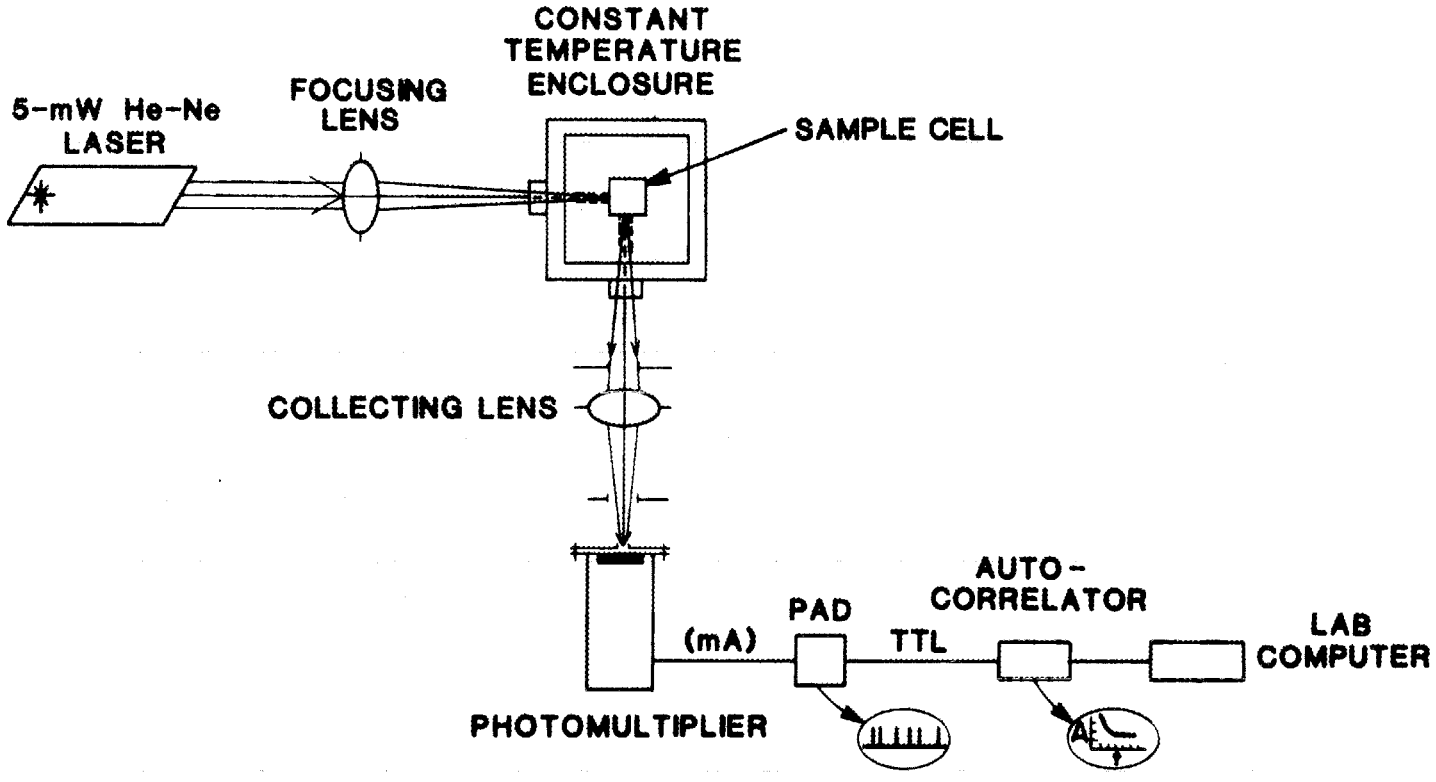

Fig. 2. Dynamic light-scattering spectrometer with auxiliary equipment for the measurement of viscosities in the subcritical region.

process the signal. The correlator is tied into an Apple IIe computer, which is programmed to control the experiment, manipulate and store the data, and calculate physical properties.

Various colloidal silicon seed solutions were added to pure liquids to create the necessary dielectric fluctuations. The liquids were placed in a teflon-coated cell, which was then placed in a temperature-controlled and insulated sample holder.

3.3 MATERIALS

For the sake of experimental convenience, only chemicals with near-ambient melting points were used. It was also necessary to choose chemicals that could be supercooled. It was found that many substances that melt in the range of 25 to 50°C crystallize immediately. The chemicals used in this study were phenol, C_6H_5OH, t-butanol, $(CH_3)_3COH$, and mutanes of t-butanol and ethanol, C_2H_5OH. Reagent grade (99 + wt % pure) fluids, which were polar and heavily hydrogen bonded, were used. Nonpolar compounds are harder to supercool and do not exhibit the same viscosity deviations as polar compounds.[1] Attempts to supercool nonpolar chemicals, such as n-docosane, $C_{20}H_{42}$, with a melting point of 44.4°C, and n-eicosane, $C_{22}H_{46}$, with a melting point of 36.4°C, failed in spite of the fact that the same procedure was used to supercool phenol and t-butanol. Impurities consisting of pure ethyl alcohol were added to t-butanol to gauge its effects on viscosity and supercooling. Ethanol was selected because of its low melting point (-114.15°C) and the similarity of its density to that of t-butanol (0.7894 g/cm3 vs 0.7860 g/cm3 for t-butanol at 20°C).

4. EXPERIMENTAL RESULTS

A number of past studies have shown that a supercooled liquid has a substantially different viscosity behavior than that exhibited by the same material above its melting point.[1–4] In many cases, the basis for asserting that the behavior of the supercooled fluid is anomalous is the fact that when one attempts to fit the data over a temperature region which passes through the melting point, a single Arrhenius correlation fails to adequately describe the behavior. On the other hand, if one fits the data above the freezing point with one Arrhenius curve and that below the freezing point with another, the data are very well described. This leads to the hypothesis that, because of the substantially higher activation energy term in the supercooled region, there must be significantly different intermolecular force fields involved in this region.

On the other hand, it has been shown that an Antoine-type correlation can be applied to data.[5] This procedure sometimes leads to a single correlation with no discontinuity in activation energy at the freezing point. A three-constant fit is involved, requiring more sophisticated nonlinear statistical routines, but these are readily available as a part of SAS, a statistical analysis program available on the laboratory's PDP 10 computer. Barlow et al.[5] found that for most of their materials, which were also polycyclic hydrocarbons, two equations were required to fit the viscosity temperature relationship around the melting point. Third constant is the correction to the temperature, which is the correction of the absolute zero to reflect viscosity behavior. Theoretically, one would expect this number to be in the region of the glass transition temperature. Therefore, this correlation would be expected to fit the data better simply by virtue of having an additional constant.

On a theoretical basis, the Antoine correlation is on weaker ground. However, a discontinuity in the viscosity behavior is also difficult to justify on any theoretical grounds. Therefore, we have opted to explore both methods of correlation in an effort to shed some light on the phenomenon.

4.1 PHENOL VISCOSITY

The viscosity of phenol (mp = 40.9°C) was measured between 22 and 70°C. As was found by earlier workers, a single Andrade correlation did not fit over the entire range of temperatures. Therefore, the data were divided at the melting point and two correlations were attempted. In the latter case, the correlation fit the data to a confidence limit which was well within experimental error. The results are shown in Fig. 3, which is a semilog plot of viscosity as a function of the inverse of absolute temperature. The intercept of the two curves is very near the melting point. The Andrade correlation is given as:

$$\mu = A \exp(B/T) \ . \tag{14}$$

The activation energy, B, increases from 3095 [K] to 3373 in crossing from above to below the freezing point. The values of the preexponential term, A, are 2.336×10^{-4} mPa•s above the freezing point and 2.747×10^{-5} below the freezing temperature. To illustrate the abrupt nature of the viscosity behavior, Fig. 4 gives a plot of the absolute deviation between the viscosity by the above-melting-point correlation and the viscosity data as a function of inverse absolute temperature. Note that deviation is almost random above the freezing point, but linearly deviated below the freezing point.

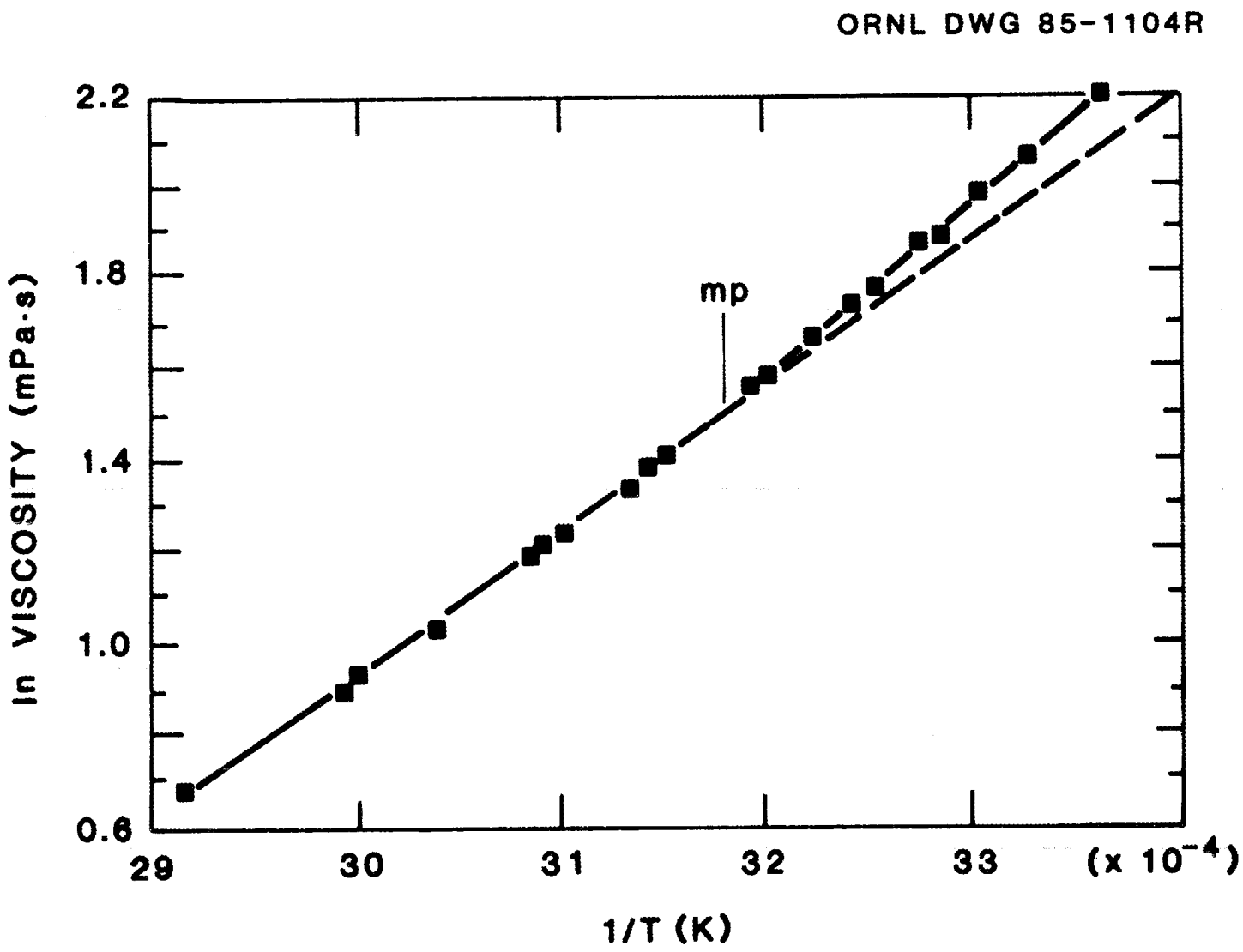

Fig. 3. Viscosity of phenol in the region of the melting point. Lines indicate the Andrade correlation fitting of the data in the two regions.

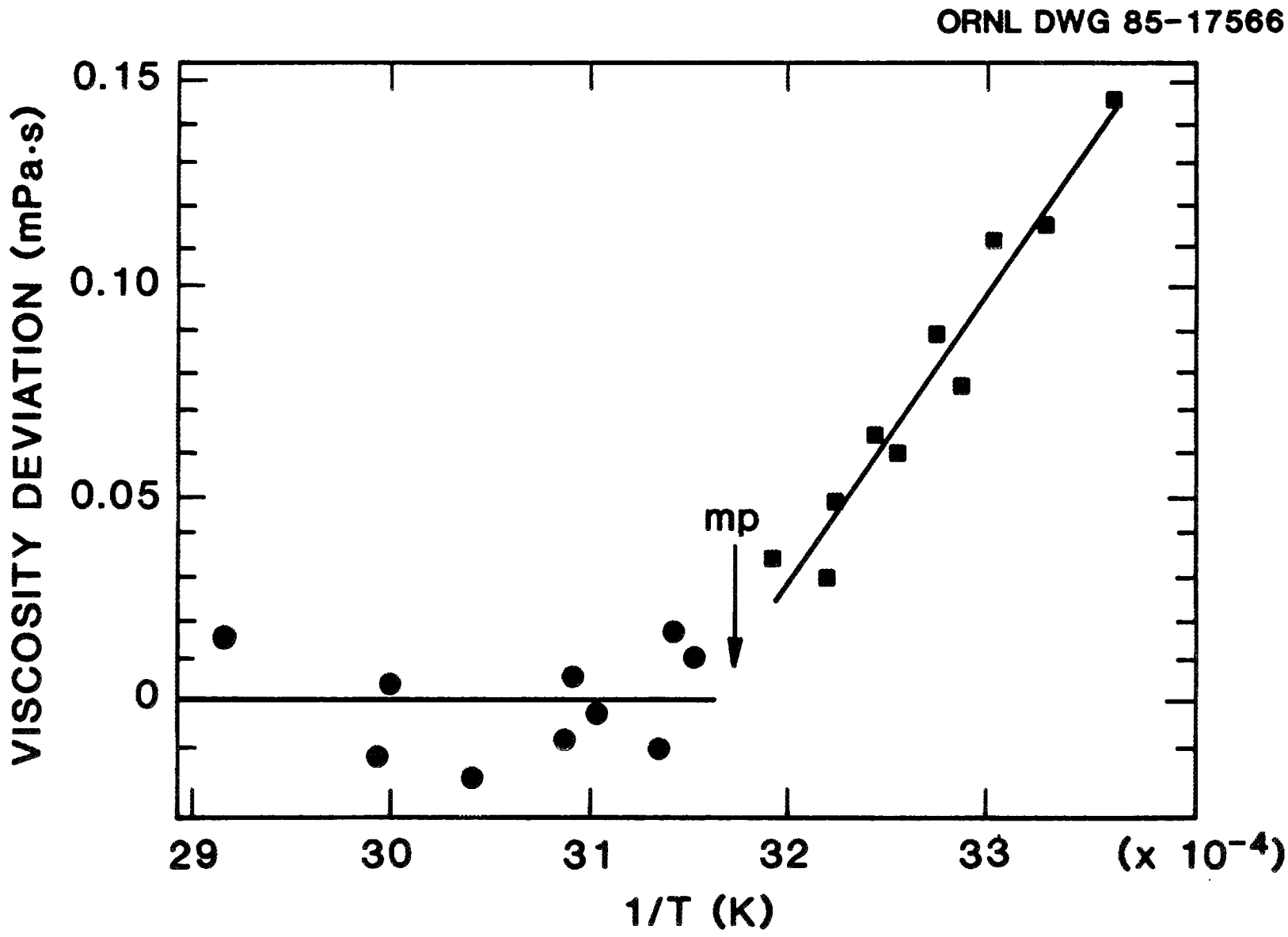

Fig. 4. Phenol viscosity data deviations from the Andrade correlation for above-melting point data.

The slope increase of 21.9% observed for phenol is of similar magnitude to the slope increases observed by Dodd and Pak of 13% for phenyl-ether. Of considerable interest is the exact point where the slope begins to change. Dodd and Pak believed that the phenomenon was strictly related to the melting point, which was substantiated by the intersection of the two phenyl-ether correlations at 26.85°C, only slightly lower than phenyl-ether's melting point of 26.95°C. They believe that the deviation point is close enough to the melting point so that it can actually be used as an accurate method of predicting the melting point without the liquid ever crystalizing. Their data on other supercooled liquids such as m-chloronitrobenzene (mP=44.29) agreed with their theory with an intersection of 44.28°C. Earlier work by Dobinski on supercooled liquid white phosphorous indicates the slope change occurs 5° above the melting point, suggesting that the effect is not completely dependent on supercooling.

The results of phenol tend to agree more with Dobinski's findings,[21] even though phenol is chemically much different from liquid phosphorous and more closely resembles the chemicals studied by Dodd and Pak. The melting point of phenol occurs at 40.9°C, yet the intersection of the two Andrade correlations puts the slope change at 43.4°C. In their extensive work, Barlow et al.[5] found that the point of intersection of the two fitted curves was in the melting point region, but there appeared to be complete randomness as concerns its exact location relative to the melting point. This is to be expected, since the basis for selecting which data are used for a given curve is arbitrary. Certainly the contention that the intersection point of the two statistical curves can be used to define the melting point is not correct, at least given the current state of data acquisition.

The Antoine correlation was fit to all of the data. The results of the correlation for all of the materials in this study are given in Table 1. As is readily apparent in Fig. 5, the single curve, which is a semilog plot of viscosity as a function of the inverse of the absolute temperature minus the correlated glass transition temperature, (Tg), fits all of the data. The fit is well within our experimental accuracy and shows no indication of any curvature in the region of the freezing point. There are no data for the glass transition for simple molecules, but in polymers, a discontinuity in the physical properties occurs at a viscosity of $\sim 10^{15}$ mPa•s. If we use the correlation we have just developed, the glass transition temperature for phenol is computed to occur at ~197.6 K. Barlow et al. found that two materials, di-n-butyl phthalate, and di-(2-ethyl hexyl) phthalate, followed the same behavioral pattern as phenol. However,

Table 1. Antoine equation constants for all materials

Mixture	A (mPa•s)	B (K)	Tg (K)
Phenol (pure)	-1.3666	269.49	-181.21
t-butanol (pure)	-4.2223	964.72	-100.00
t-butanol (0.06% ethanol)	-4.1725	940.00	-103.00
t-butanol (0.6% ethanol)	-3.878	880.00	-103.00
t-butanol (1% EtOH)			
All data	-3.878	880.00	-103.00
Low-temperature	-4.235	950.00	-103.00
High-temperature	-3.852	875.00	-103.00

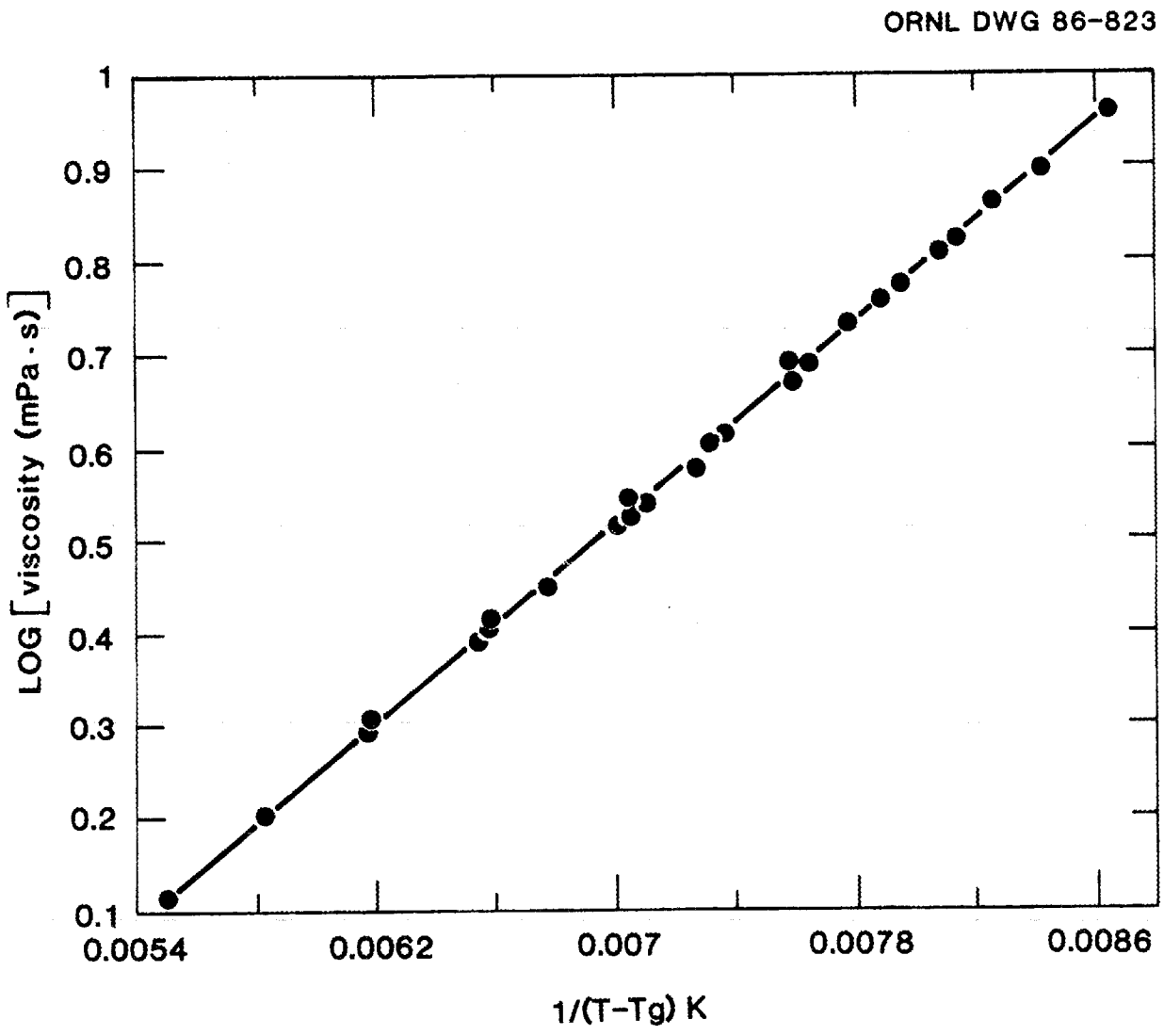

Fig. 5. Antoine relationship for pure phenol [(A = -1.366) (B = 269.48 K) (Tg = -181 K) (xx data — correlation)].

the remaining eight substances which they studied required two Antoine-type curves to describe the viscosity behavior in the freezing point region. A great deal of significance is not ascribed to this fact, since one would certainly arrive at a slightly different set of fitting parameters if one chose to divide our phenol data into two regions at the melting point. The important conclusion must be that the viscosity behavior in the freezing point region does not match the simple Andrade relationship, but the onset of longer range associations in the liquid gives rise to a more complex relationship. In the case of phenol, this may be described either by a single Antoine-type curve or by two Andrade correlations, with the intersection point very close to the freezing point.

4.2 TERTIARY BUTANOL DATA

The viscosity of pure tertiary butyl alcohol was measured above and below the melting point in the same manner as was phenol, with similar results (Fig. 6). A linear regression fit of the data produced two significantly different sets of Andrade coefficients. The data were compared with the normal liquid Andrade correlation, and the deviations were plotted against the inverse of absolute temperature. The resulting graph (Fig. 7) is similar to that of phenol (Fig. 4) and emphasizes the magnitude of the supercooled viscosity change. The slope increase of 18.8% was similar to that observed in phenol, yet the temperature at which the slope breaks (26.02°C) was much closer to the melting point of the chemical, 25.66°C, than that observed with phenol.

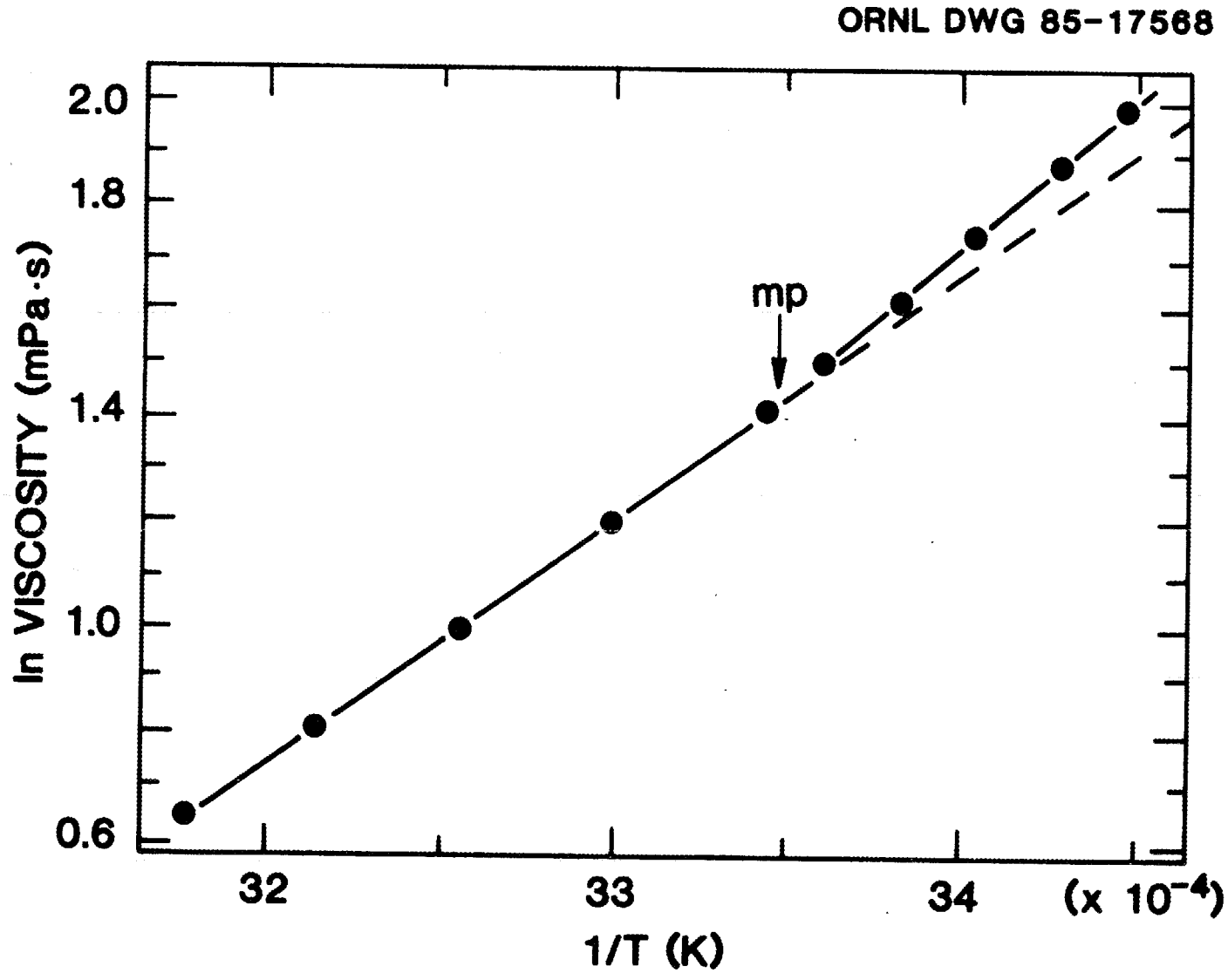

Fig. 6. Viscosity of pure t-butanol in the region of the melting point. Lines indicate the Andrade correlation fitting of the data in the two regions.

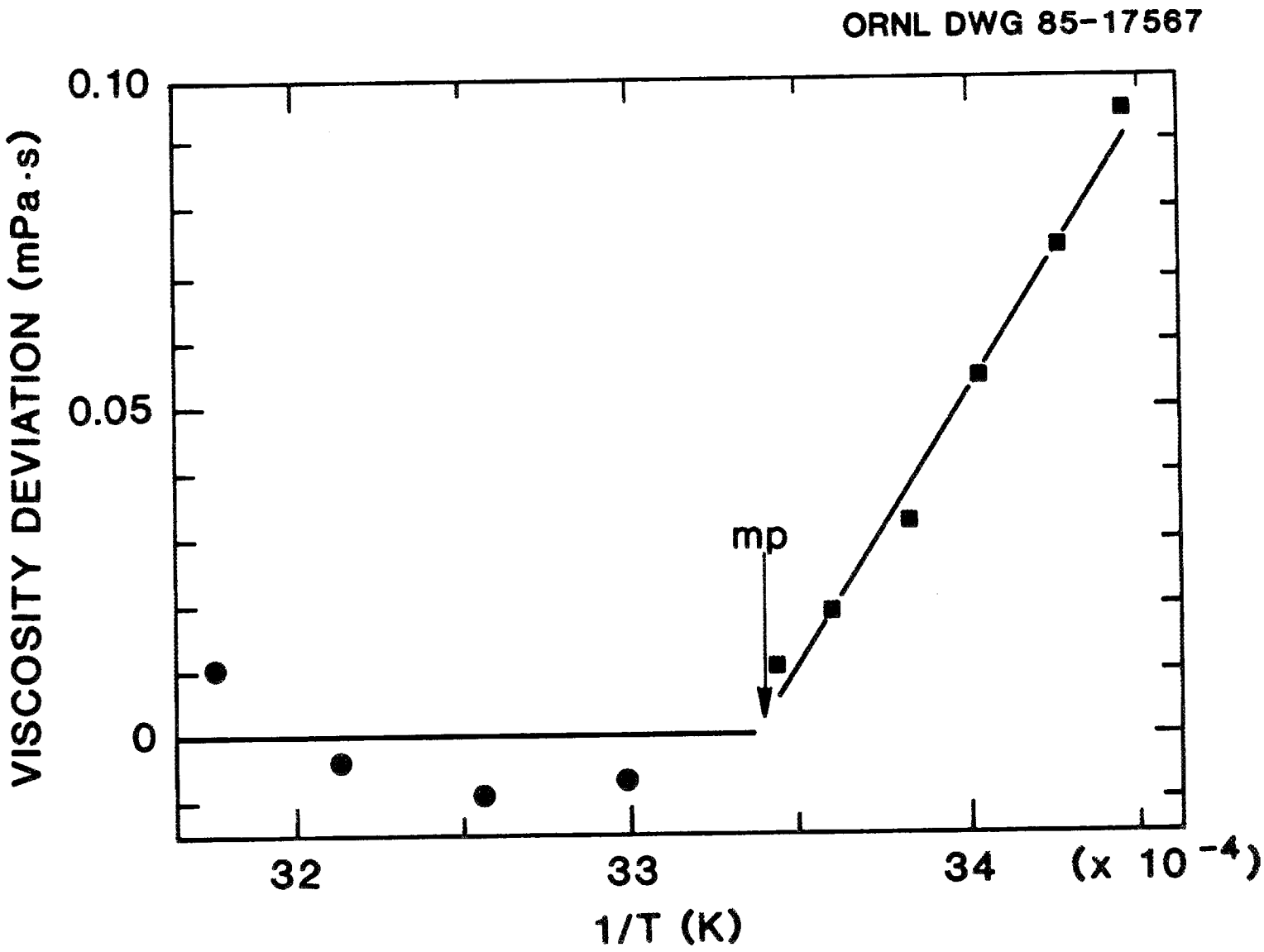

Fig. 7. Pure t-butanol viscosity data deviations from the Andrade correlation for above-melting-point data.

Again, all the viscosity data for pure t-butanol were analyzed using an Antoine-type equation. The results (Fig. 8) indicate that one might be justified in accepting this fit as being within the experimental error of the method. However, there appears to be a slight difference in the slope above and below the melting point. This "knee" was investigated in association with some of the other t-butanol viscosity analysis and found to be a slight, but definite, effect. Much more data would be required than are available to give a definitive evaluation of this point.

Minute amounts of ethyl alcohol were added to tertiary butyl alcohol in order to gain further insight into the relationship between viscosity change and melting point. The small quantities of ethyl alcohol added, 0.06, 0.6, and 1% by weight, were added with the intention of altering the mixture melting point without significantly altering the liquid's density or viscosity. The resulting mixtures were observed to melt at temperatures slightly below 20°C, at least 6 degrees below the normal melting point of t-butanol. As expected, the more viscous ethyl alcohol slightly raised the viscosity of the t-butanol, yet the viscosity deviations observed remained similar to those observed in pure t-butanol.

The viscosities of the three t-butanol mixtures (0.06, 0.6, and 1% EtOH) were measured both above and below the normal melting point of pure t-butanol. As with pure t-butanol and phenol, the data produced two distinct Andrade correlations with substantial increases in the B coefficients (Figs. 9, 10, 11). The slope changes occurred not at the actual liquid's melting point (below 20°C) but at ~1 to 4° above the melting point of pure t-butanol. The Andrade constants, slope changes, and slope deviation points are listed for pure t-butanol and its mixtures with ethanol (Table 2).

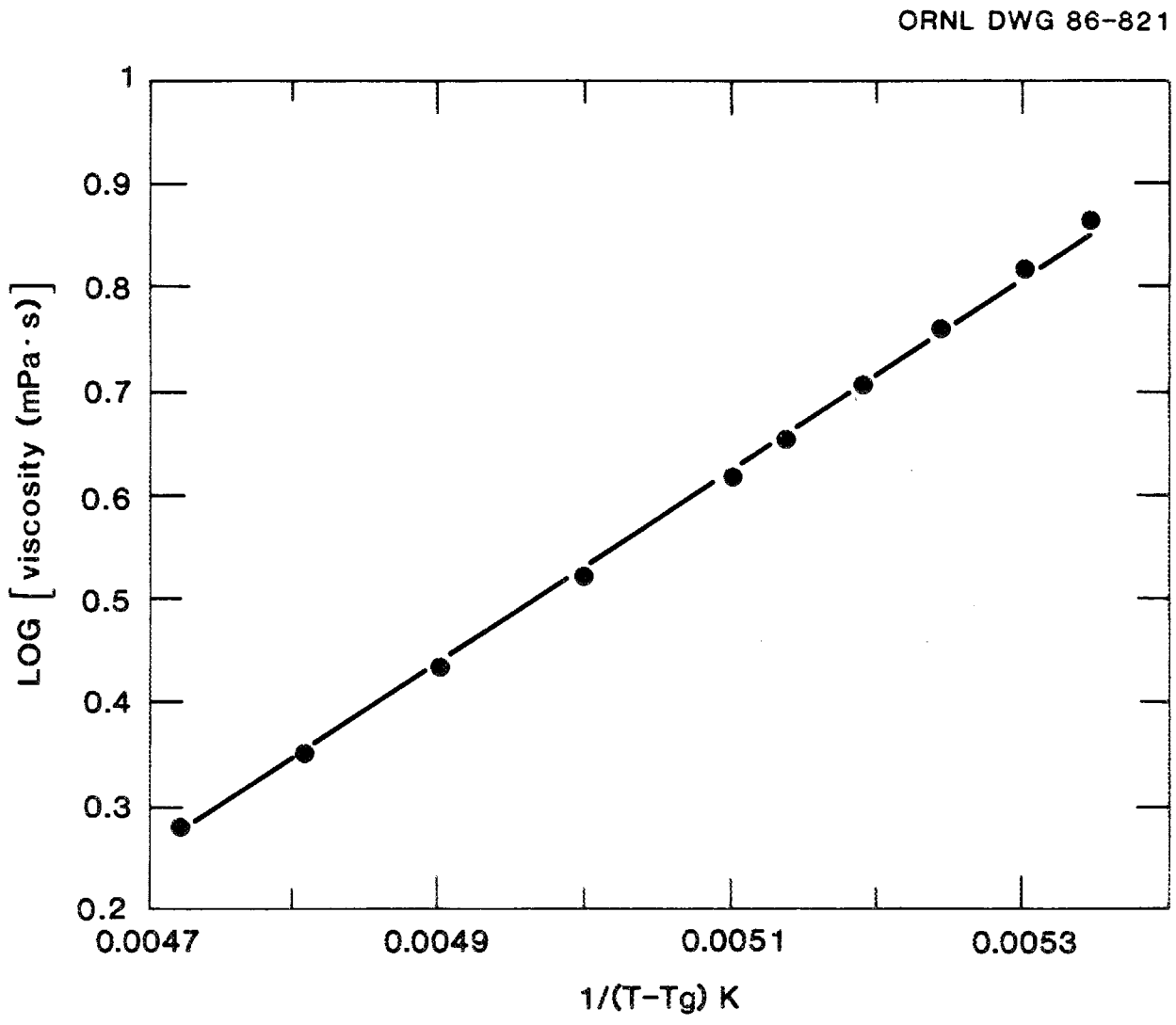

Fig. 8. Antoine relationship for pure t-butanol [(A = -4.06922 mPa•s) (B = 920 K) (Tg = -103 K) (xx Data — correlation)].

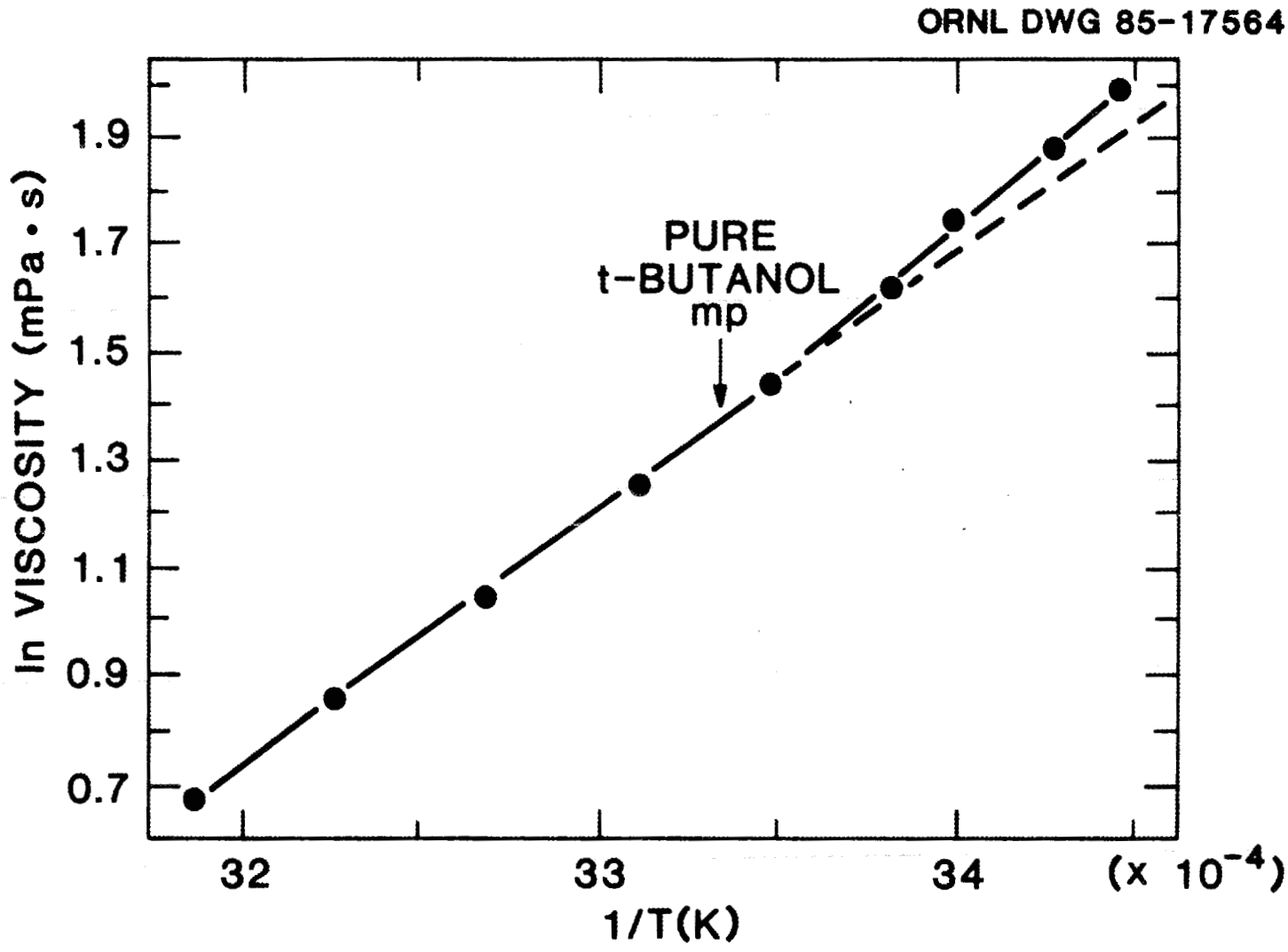

Fig. 9. Viscosity of pure t-butanol containing 0.06 wt % ethanol in the region of the mixture melting point. Lines indicate the Andrade correlation fitting of the data above and below the pure t-butanol melting point.

ORNL DWG 85-17569

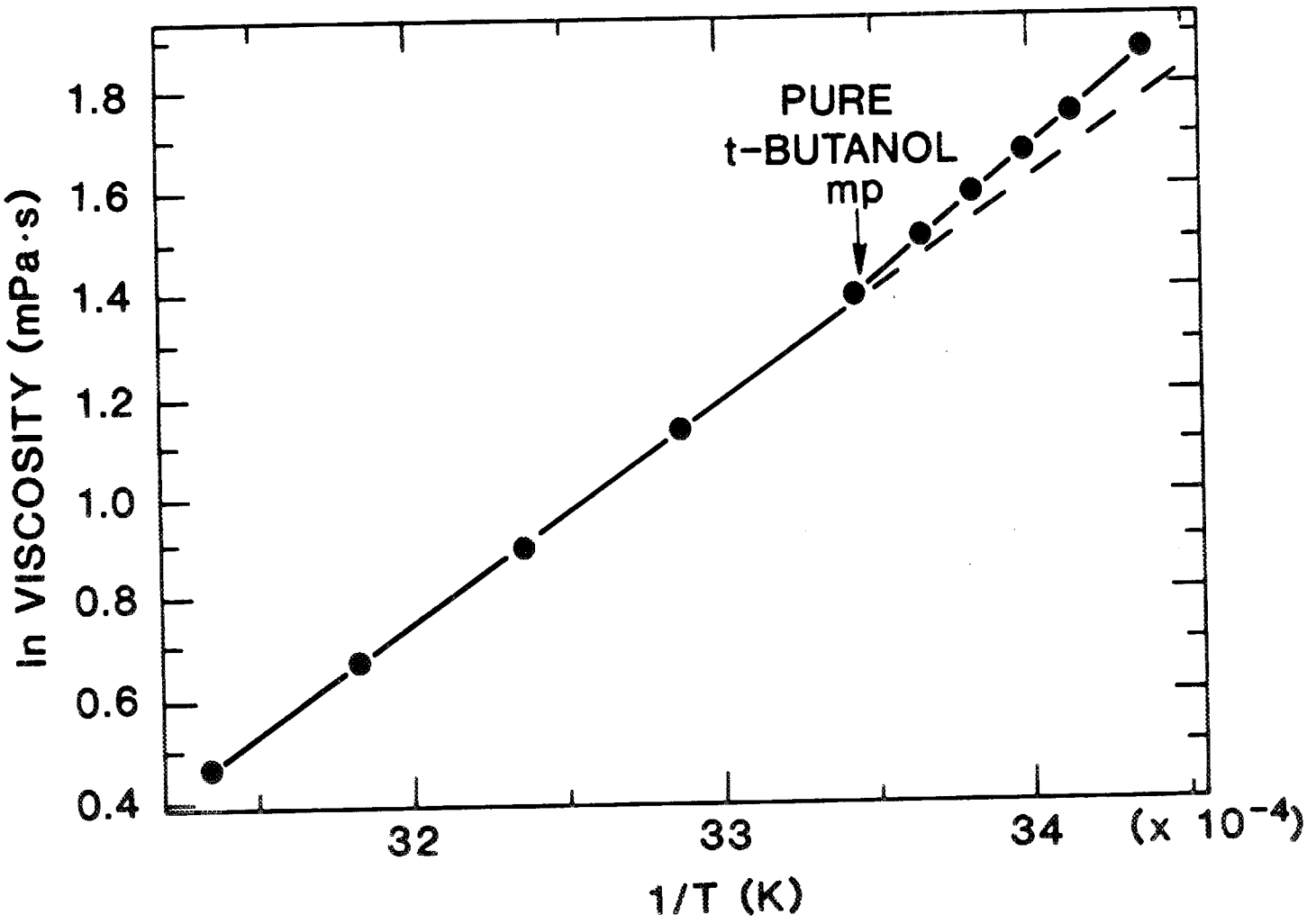

Fig. 10. Viscosity of pure t-butanol containing 0.6 wt % ethanol in the region of the mixture melting point. Lines indicate the Andrade correlation fitting of the data above and below the pure t-butanol melting point.

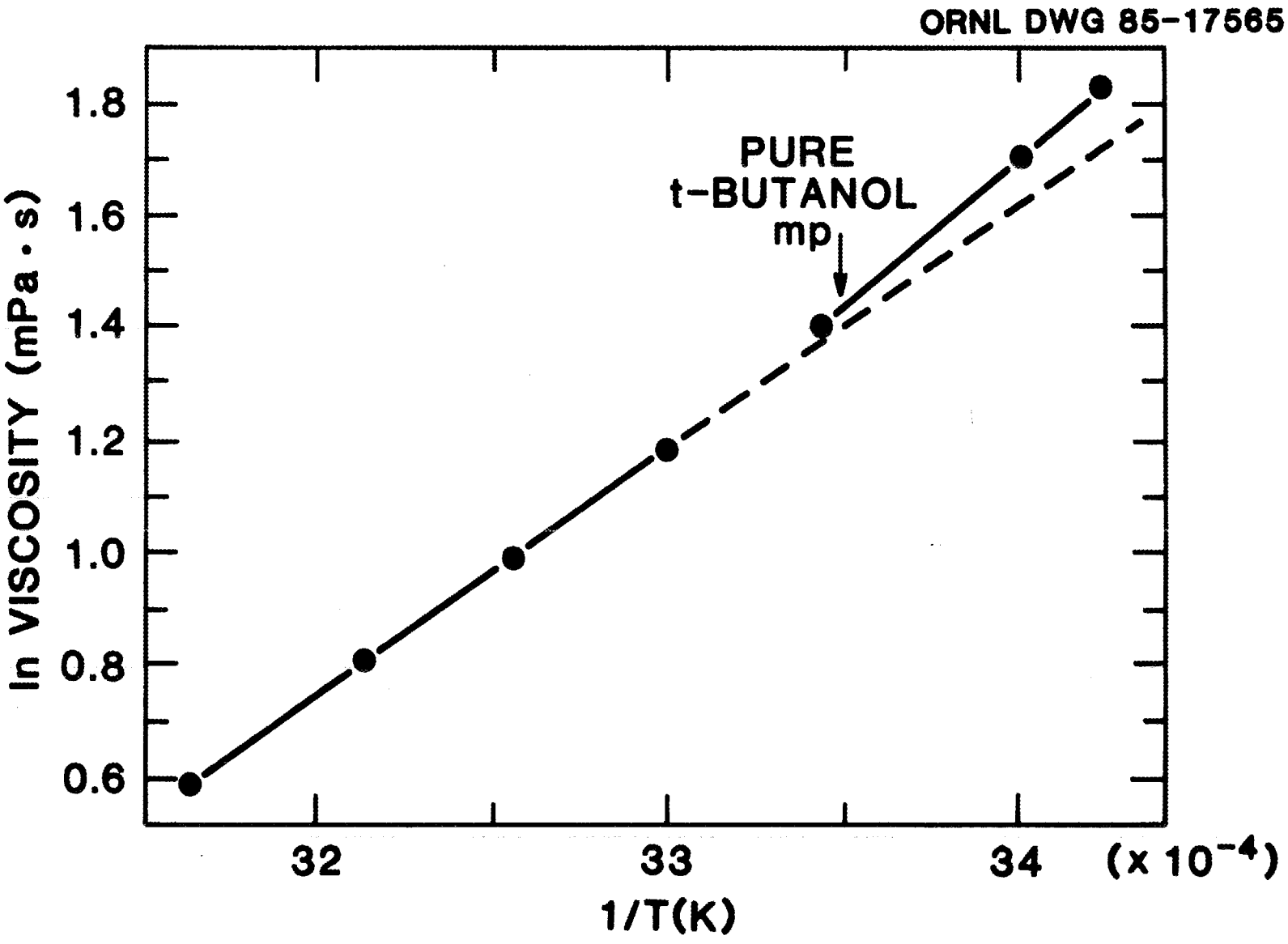

Fig. 11. Viscosity of pure t-butanol containing 1.0 wt % ethanol in the region of the mixture melting point. Lines indicate the Andrade correlation fitting of the data above and below the pure t-butanol melting point.

Table 2. Viscosity correlation data for t-butanol

Compound	Melting point (°C)	Temperature range (°C)	Andrade constants: Above melting point A[mPa•s]	Above melting point B[K]	Deviated A[mPa•s]	Deviated B[K]	% change in B	Temperature of B change	Coefficient of determination normal	Coefficient of determination deviated
Pure t-butanol	25.66	17-42	7.287×10^{-7}	4648	3.9308×10^{-8}	5522	18.79	26.02	0.99959	0.99981
0.06% EtOH-t-butanol	<20	17-42	6.835×10^{-7}	4667	3.98×10^{-8}	5518	18.22	25.99	0.9992	0.99991
0.6% EtOH-t-butanol	<20	17-42	2.468×10^{-6}	4269	2.073×10^{-7}	5019	17.56	29.53	0.99924	0.99947
1% EtOH-t-butanol	<20	17-42	1.697×10^{-6}	4387	1.080×10^{-7}	5216	18.98	28.85	0.99941	0.99998

Antoine-type curves were developed for all mixtures, being quite similar to the one developed for pure t-butanol. The constants are given in Table 1. The data indicate a slight difference in slope (~10%) in the log 10 (viscosity) as a function of the inverse of absolute temperature minus a fitted glass transition temperature [1/(T - Tg)]. As an example, the 1% ethanol- t-butanol mixture data were correlated with both one and two curves (Fig. 12). There is a better fit of the data in the two-curve case, but it is probably moot, since the data base is too sparse to make definitive judgments.

4.3 VISCOSITY TIME DEPENDENCE

If a structural change is responsible for the viscosity deviations seen in phenol and t-butanol, it is possible that the degree of structural change varies with time. A sample of t-butanol with 0.06% EtOH was kept at a constant temperature for a period of 24 h while its viscosity was measured at regular intervals. Initially, the liquid was held at 20.91°C, ~8°C below the observed viscosity slope deviation point. The viscosity of the chemical was observed to undergo a small but steady decrease with time (Fig. 13). The same chemical, when held at a temperature above the viscosity deviation temperature, showed no noticeable change in viscosity.

A similar set of experiments were performed on supercooled and normal liquid phenol with similar results: supercooled phenol underwent a steady small decrease in viscosity (Fig. 14). The viscosity of phenol held at 46.65°C showed only an insignificant decrease as compared with the decrease exhibited by supercooled phenol.

ORNL DWG 86-822

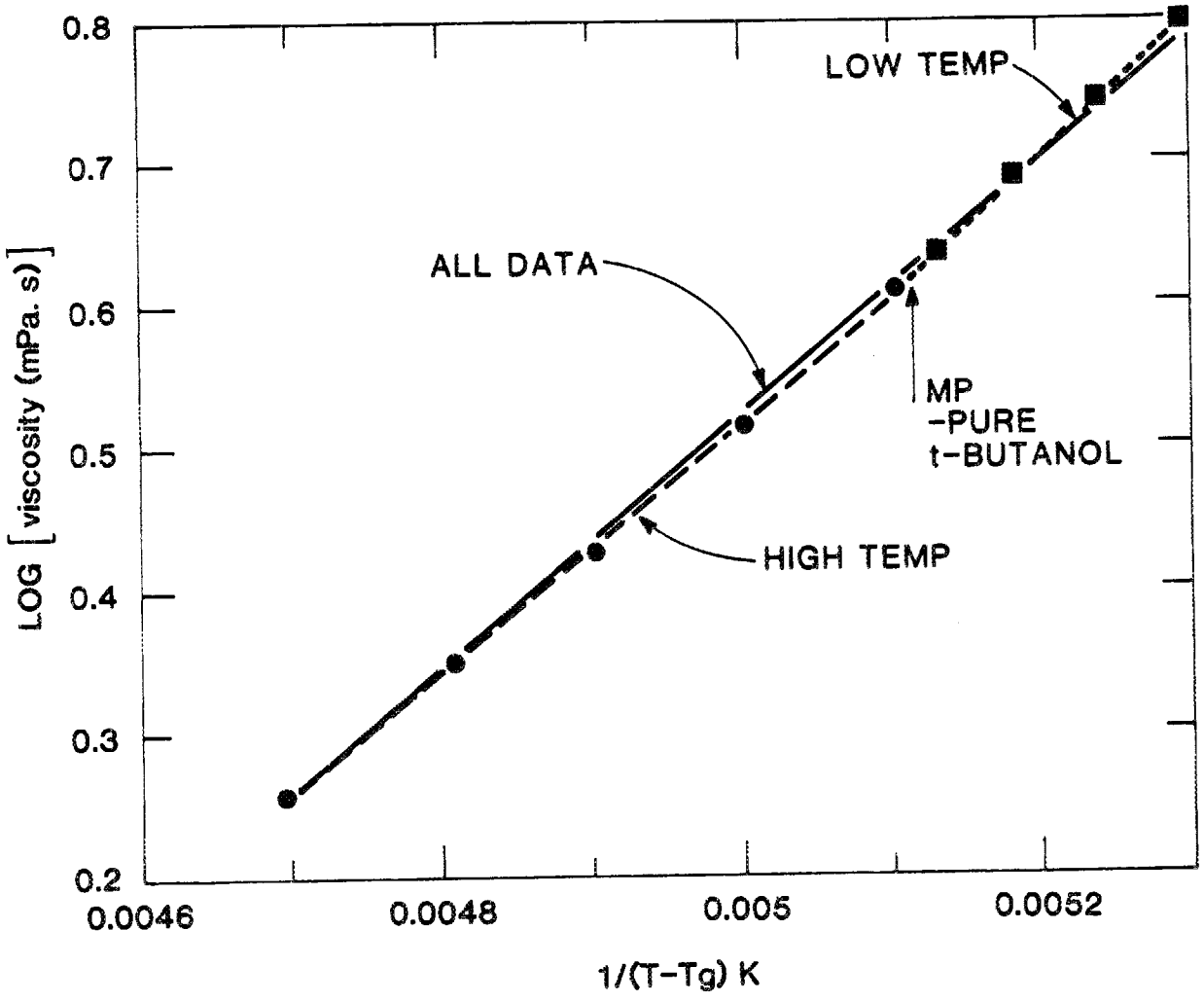

Fig. 12. Antoine relation for t-butanol containing 1% ethanol [(x data) (— correlation all data) (– – – high-temperature correlation) (---- low-temperature correlation)].

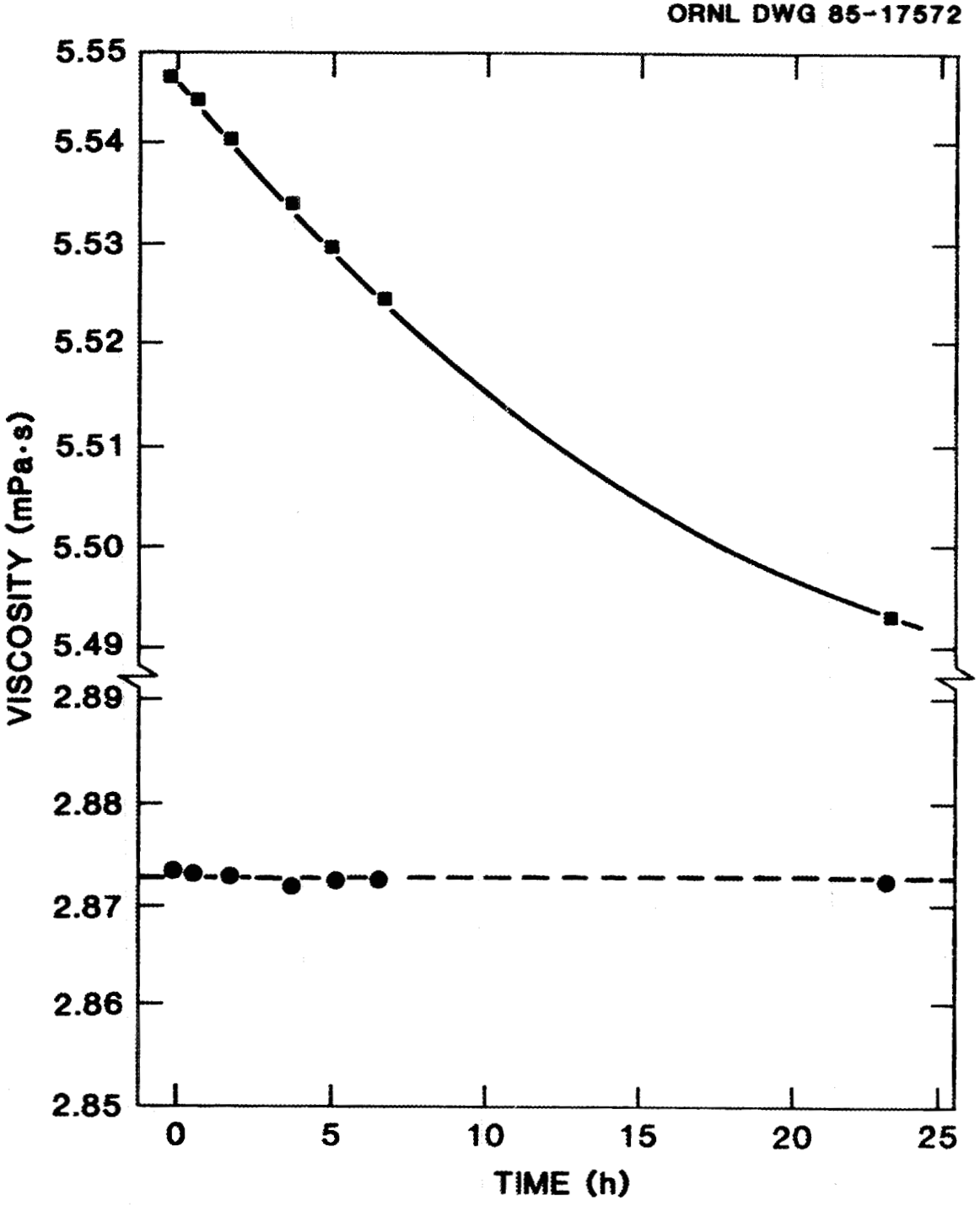

Fig. 13. Viscosity functionality in time for the t-butanol –0.06% ethanol system above and below the normal boiling point (■ – below freezing; ●●● – above freezing).

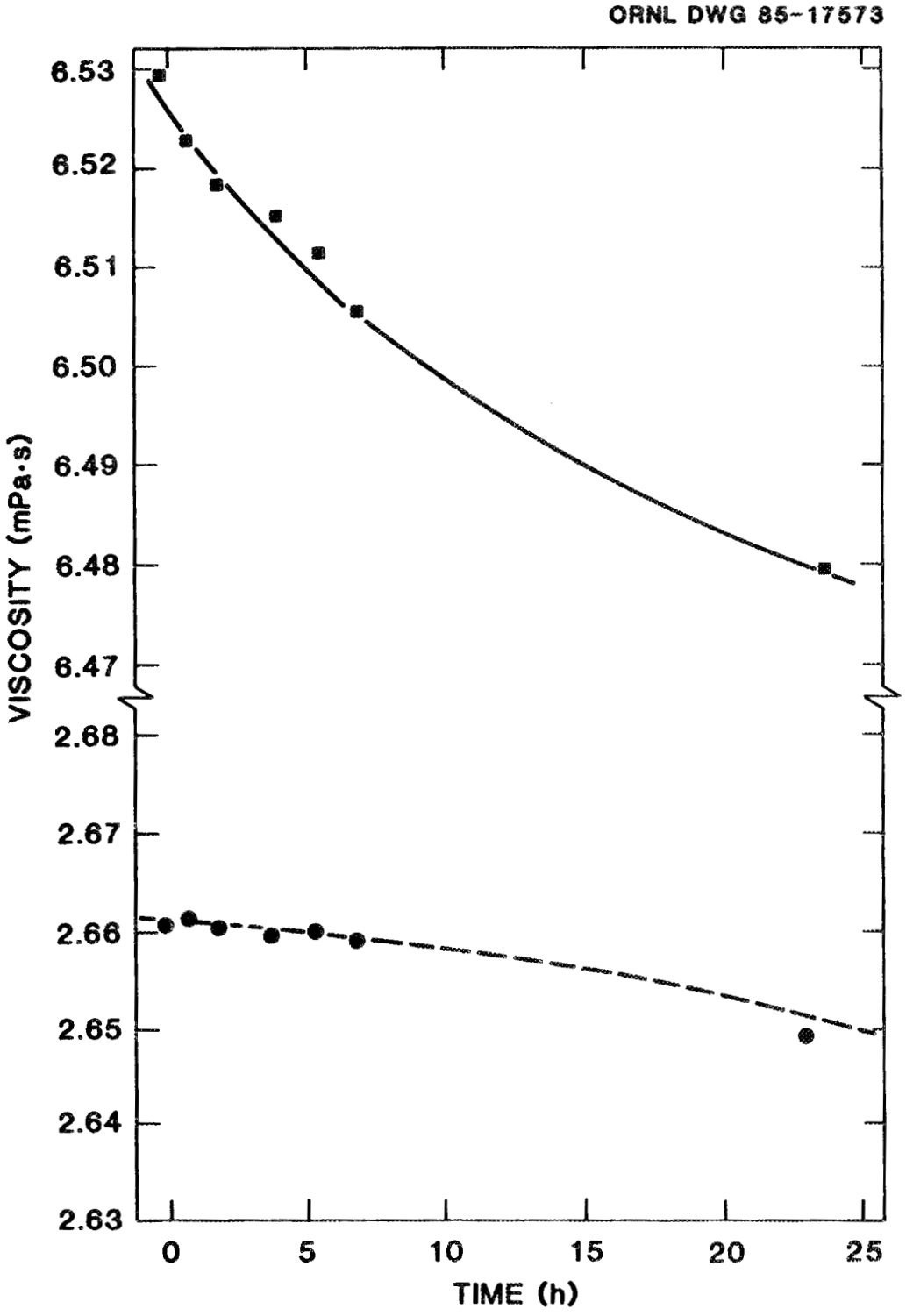

Fig. 14. Viscosity functionality in time for pure phenol above and below the normal boiling point (■ - below freezing point; ● - above freezing point).

4.4 LASER LIGHT-SCATTERING STUDIES

There are a number of reasons for using a totally different approach to the measurement of supercooled viscosities. Foremost is the fact that most of the data in this area have been obtained with capillary viscometers. If there is an artifact, such as local crystallization in the wall area, associated with the performance of the capillary viscometer, effectively reducing the radius of the tube and thus resulting in spuriously high measurements, one has no way of filtering this fact from the experiments, causing a changing mixture with time. The laser-scattering method was selected as the alternate method, because values are inferred from a point well within the mass of the fluid and are dependent upon Brownian motion. On the negative side, it is necessary to introduce a submicron seed material into the mass of fluid. Pure phenol and t-butanol were repeatedly introduced with silica seed particles and studied with the laser light apparatus described earlier.

Pure phenol was examined using laser light scattering in an attempt to confirm the existence of crystals or molecular aggregates. The material was supercooled without any seed in a laser light-scattering apparatus and monitored periodically for the occurrence of any agglomerates. The results were characteristic of a completely homogeneous mixture; however, the laser used is only powerful enough to detect particles 0.03 μm in diam. Eventually, after days of observation, the mass would crystallize almost instantaneously, without any observable change in the fluid right up to the time of crystallization. It has been shown both theoretically and through inferential experimentation that agglomerates do indeed precede the crystallization process. Current crystallization

theory by Mullin suggests that the agglomerates are ~0.005 μm in diam.[22] This would require a much better instrument before we could detect the onset of agglomeration.

5. DISCUSSION

The Andrade correlation, which is based upon relatively firm theoretical ground, is only applicable at temperatures well removed from the melting point. In this region one must fit data with two curves, one above and one below the melting point of the pure substance. On the other hand, the Antoine equation tends to pass through the melting point of some substances, such as phenol, continuously. This is expected since there is an additional parameter in the equation. Here the theoretical ground is somewhat shakier, but the added parameter is described as a characteristic temperature, below which viscosity fails to have a significant meaning (above 10^{-15} mPa•s). Even with this equation, we and other workers have found many cases where two Antoine equations are needed to describe the behavior of viscosity in the region of the melting point. There is, therefore, a significant increase occurring in the intermolecular force field in the melting point region. This is possible due to the combined effects of longer-range intermolecular potentials and the formation of agglomerates. In the supercooled region, where the situation becomes metastable, one would expect an extension of that tendency, and, therefore, this is a particularly productive area in which to study viscosity behavior. The magnitude of the change is sufficiently large to indicate a major structural change, yet such a change has yet to be demonstrated directly. To emphasize the extent of the change in activation energy, Dodd and Pak cite the change in slope occurring

between $CH_3-O-C_3H_7$ and its isomer $C_2H_5-O-C_2H_5$.[4] The major structural change between isomers causes a change in Andrade B values of only 1.3%, less than one-tenth of the change observed with phenol and t-butanol passing their viscosity deviation point. Greenwood showed increases in the value of B ranging from 7.9 to 27.4% on supercooling various chemicals, with the change increasing with the increasing chain length of the particular chemical.[3]

The structure of the supercooled state could be conjectured to be similar to the liquid above its melting point but with some of the longer-range order, perhaps in the form of clusters, which is characteristic of the solid state. It is important that this form be studied, because it is during the time when a fluid is in a supercooled state that it begins the solidification process and acquires its crystal habit. The development of a theory on the structural change of supercooled liquids first requires a theory of the liquid structure. Furth[23] describes the rapid increase of supercooled Andrade B values in terms of a "hole theory" of the liquid state. The liquid structure is characterized by the presence of holes whose size distribution depends on temperature and pressure. Viscosity is postulated to be the result of the momentum transfer by the Brownian movement of the holes, which is consequently dependent on the magnitude, mean free path, and mean lifetime of the holes. Furth suggests that the energy term in the Andrade equation is the product of the molecular work function for the vaporization of a molecule to form holes and z, the number of molecules neighboring the hole. The Andrade energy term exhibits a sharp increase in the supercooled region. Furth has shown that there is a substantial increase in the number of holes, which serves to

increase the molecular work function. Since the total energy does not change during supercooling, z must drop abruptly at the supercooling point, which would represent a substantial change in structure. According to Furth, his calculations predicting the drop in z and rise in d agreed with the viscosity data for phenyl ether.

Andrade[1] proposes a similar theory to explain the observed phenomenon. His hypothesis is that the increase in viscosity is due to the fluctuating formation of small crystalline nuclei. Greenwood[3] cites a past experimental correlation as evidence of the crystalline or molecular aggregation theory. Batchinski[24] showed that viscosity could be related to specific volume in many cases by the equation

$$V = b + B\phi \ ,$$

where $\phi = 1/\mu$, the fluidity, and b and B are experimentally fitted constants. By taking the derivative of the equation, the following results:

$$B = \frac{\delta V}{\delta \phi} \ .$$

Experiments by Greenwood[3] and Dodd and Pak[4] have shown no evidence of a density shift, and therefore, of a specific volume shift, when a liquid passes into a supercooled state. With this in mind, Greenwood has found that a plot of ϕ vs specific volume reveals a linear relationship both above and below the melting point of various substances, yet with different slopes (B values) for each region. Since B is assumed proportional to size of flow units, this suggests a level of enhanced molecular aggregation as a liquid is passed into the supercooled region. Recent

work by Mullin[22] further suggests the existence of very small crystalline clusters dependent on a variety of factors, including impurities, temperature, and pressure.

Given that there is considerable evidence of cluster formation in supercooled liquids, both from viscosity and crystallization theory approaches, it would be a natural evolution of this program to seek these important precursors to crystallization. Based upon his theory, Mullin has predicted that the clusters should be ~50 Å in diam, a size which is on the edge of the resolution of a good research laser light-scattering apparatus. Although our initial attempts in this area met with no success, it remains a good approach for the future.

The temporal change in viscosity is more questionable. While the observed changes are small, they are within the limits of the experimental accuracy of the method. Further, they have been repeated and tend to occur with the two systems which we studied for the effect for this phenomenon. Certainly more verification is demanded, but if we assume for the present that we are indeed observing something fundamental rather than an experimental artifact, some explanation is required. In supercooled fluids, crystallization will eventually occur. Thus, we can expect change with time in the characteristics of the material leading to crystallization, rather than an incubation period followed by a discontinuous event. Largely increasing order would imply increasing viscosity with time, which is the opposite to the result at hand. If, on the other hand, the clusters were denser than the medium and sedimented to the bottom of the reservoir bulb, one would use viscosity samples which are more characteristic of the fluid as time progressed.

This would give a decreasing viscosity measurement. This model is somewhat flawed because of the fact that there was considerable agitation associated with the measurement, and, thus, one would expect a great deal of variation in the measurements. This was not observed — the decline in viscosity was very regular. Again, here, a means of observing the clusters might produce some fascinating results.

It is not possible to measure supercooled viscosities for a large number of fluids. As a part of the current study, we attempted to supercool two long-chain hydrocarbons, eicosane (C_2OH_{42}) and docosane ($C_{22}H_{46}$). They crystallized immediately upon passing through their freezing temperature. Therefore, it was concluded that the type of internal order that exists in the fluid determines whether subcooling is possible. Heavily hydrogen-bonded substances, aromatics, and materials with some impurity appear to be the best candidates for such studies.

6. CONCLUSIONS

The following conclusions may be drawn from these studies:

1. If one chooses to correlate viscosities of liquids near the melting point with the Andrade correlation, two curves are read to fit the data, one point above the melting point, and the other below.
2. When drawn on the same coordinate axes, the two straight-line fits of the data in the two regions intersect very close to the normal melting point of the compound, in the case of pure materials, and very close to the melting point of the material which is below its melting point, in cases where a mixture is involved. The change in activation energy associated with the supercooled region is observed in pure phenol, pure t-butanol, and ethanol-t-butanol mixtures,

suggesting that some type of structural change is taking place at temperatures near the melting point.

3. The Antoine correlation may be used to fit both phenol and t-butanol data with a single continuous curve throughout the region.
4. Attempts to observe the viscosity behavior in the supercooled region using seeded media resulted in growth of the seeds, presumably as a result of precipitation on the seed particles. This, of course, rendered the results invalid.
5. There is a slight but measurable decrease in viscosity with time in the supercooled region, which is not observed in the region above the melting point. This conclusion requires reconfirmation.

7. RECOMMENDATIONS

1. Supercooled data with nonpolar materials would be of interest because of the entirely different nature of the bonding in such systems. This will probably require the inclusion of impurities.
2. To date, we have measured the viscosity behavior of mixtures in which a single component (the more concentrated one) is below its melting point. The supercooled viscosity curve indicates that the curve intersects the above-melting viscosity curve at the melting point of the pure compound which is supercooled. Mixtures in which both materials are supercooled are of considerable interest.
3. Correlation work will be required as a greater body of literature accumulates in the area.
4. Unseeded laser light-scattering work in which one uses low-angle scattering may allow one to observe clusters.

8. REFERENCES

1. E. N. da C. Andrade, "Viscosity of Liquids," Proc. Phys. Soc. A-215, 36-43 (1952).

2. F. C. Frank, "Supercooling of Liquids," Proc. Phys. Soc. A-215, 43-46 (1952).

3. N. N. Greenwood and R. L. Martin, "Discontinuities in the Properties of Supercooled Liquids," Proc. Phys. Soc. A-215, 46-65 (1952).

4. C. Dodd and Hu Pak Mi, "Viscosity and Density in the Supercooled Liquid State," Proc. Phys. Soc. B-62, 454-60 (1949).

5. A. J. Barlow, J. Lamb, and A. J. Matheson, Proc. R. Soc. A 292, 322 (1966).

6. A. E. Clark and T. A. Litowitz, J. Acoust. Soc. Am. 32, 1221 (1960).

7. G. Harrison, The Dynamic Properties of Supercooled Liquids, Academic Press, London, 1976.

8. R. B. Bird, W. E. Stewart, and E. N. Lightfoot, Transport Phenomena, John Wiley & Sons, Inc., New York, 42-48, 1960.

9. R. C. Reid, J. M. Prausnitz, and T. K. Sherwood, The Properties of Gases and Liquids, 3rd ed., McGraw-Hill, New York, 435-69, 1977.

10. G. S. Fulcher, J. Am. Ceram. Soc. 8, 30 (1925).

11. G. Tammann and W. Hesse, Z. Anorg. Allg. Chem. 156, 245 (1926).

12. A. K. Dolittle and D. B. Dolittle, J. Appl. Phys. 28, 901 (1957).

13. M. H. Cohen and D. Turnbull, J. Chem. Phys. 31, 1164 (1959).

14. T. A. Litowitz, J. Chem. Phys. 20, 1088 (1952).

15. A. J. Barlow and J. Lamb, Proc. R. Soc. A253, 52 (1959).

16. J. R. Van Wazer, J. W. Lyons, K. Y. Kim, and R. E. Colwell, Viscosity and Flow Measurement, Interscience Publishers, New York, 1963.

17. D. F. Williams, C. H. Byers, and C. R. Young, Viscosities of Polyaromatic Hydrocarbons: Experiments and Prediction, ORNL/TM-9410, Oak Ridge National Laboratory, Oak Ridge, Tennessee, June 1985.

18. American Society for Testing and Materials, ASTM-D446-79, Standard Specifications and Operating Instructions for Glass Capillary Viscometers, 1979.

19. American Society for Testing and Materials, ASTM-D445-79, Standard Test Method for Kinematic Viscosity of Transport and Opaque Liquids, 1979.

20. D. F. Williams, C. H. Byers, and J. S. Watson, Determination of High-Temperature Fluid Viscosity Using Dynamic Light Scattering, ORNL/9648, Oak Ridge National Laboratory, Oak Ridge, Tennessee, August 1986.

21. S. Dobinski, Bull. Int. Acad. Cracovie B-4A, 103 (1934).

22. John W. Mullin, "Nucleation and Crystal Growth," Chem. Ind. 9, 372-77 (May 1980).

23. R. Furth, Proc. Phys. Soc. 52, 768 (1940).

24. A. J. Batschinski, Z. Phys. Chem. 84, 643 (1913).

25. J. Timmermans, Physico-Chemical Constants of Pure Organic Compounds, Elsevier Publishing Company, Inc., New York, 1950.

APPENDIX A

APPENDIX A

The basic measurement made in the current study is the kinematic viscosity (in centistokes), although viscosity in centipoise is more useful in most applications. The relationship between the two quantities is given by the following equation:

$$V = \frac{\mu}{\rho} , \qquad \text{(A-1)}$$

where ρ is the density of the medium. Since the specific gravities of the media of the fluids vary considerably with temperature, it is important to measure or predict density at each experimental temperature. For pure fluids, density follows a linear relationship with temperature. It might be expected that this linear relationship changes in the supercool region similar to the viscosity change, yet experiments by Andrade, Dodd and Pak, and Greenwood have found density to follow the same linear relationship above or below the melting point. Density measurements were made using a Mettler/Par DMA 55 precision densitometer. A linear regression curve fit of the measured data, along with published literature values,[25] produced the following density equation:

$$\rho = -8.81514 \times 10^{-4} \cdot T + 1.09427 , \qquad \text{(A-2)}$$

where T = temperature in degrees C.

A similar procedure produced a density equation for the tertiary butyl alcohol used:

$$\rho = -1.0535 \times 10^{-3} \cdot T + 0.807775 . \qquad \text{(A-3)}$$

The density of the ethanol-t-butanol mixtures was assumed to be the same as that for pure density due to the minute amounts and similar densities. (EtoH @ 20°C, 0.7894, t-butanol @ 20°C, 0.7860).

APPENDIX B

APPENDIX B

This section contains the experimental data obtained in this study. Included are average temperature, the kinematic viscosity, the dynamic viscosity, and the coefficient of variation among the replicate runs (generally five). The viscosity in centipoise is the product of the viscosity in centistokes (measured directly) and the density calculated from the linear equations fitted from known data.

Table B.1. Viscosity data

Average temperature (°C)	V (Cst)	μ (CP)	Coefficient of variation (%)
	Pure phenol		
50.0	3.23	3.3921	0.03
59.99	2.44	2.5410	0.04
69.98	1.90	1.9620	0.10
60.0	2.44	2.54096	0.04
44.76	3.81	4.0188	0.01
29.13	6.8306	7.2991	0.01869
48.98	3.3018	3.4694	0.02077
43.92	3.8803	4.0947	0.007835
38.88	4.6164	4.8922	0.01129
33.81	5.5801	5.93981	0.0047
60.79	2.3490	2.4445	0.0209
55.74	2.6804	2.8014	0.0179
50.695	3.1202	3.2749	0.00682
45.635	3.60599	3.8009	0.0200
39.94	4.4810	4.7457	0.0547
34.87	5.4081	5.7517	0.0471
30.83	6.2365	6.6550	0.03665
26.815	7.4069	7.9300	0.00837
23.775	8.5151	9.1393	0.00684
31.79	6.1240	6.5297	0.0907
36.635	5.10277	5.41900	0.0281

Table B.1 (continued)

Average temperature (°C)	V (Cst)	μ (CP)	Coefficient of variation (%)
	t-butyl alcohol		
24.505	5.7533	4.4988	0.0229
22.485	6.4771	5.0786	0.02153
20.505	7.3094	5.7465	0.01268
18.48	8.3144	6.5543	0.01317
16.87	9.2544	7.3110	0.0231
25.87	5.3085	4.1434	0.00491
29.875	4.2774	3.3205	0.03445
33.87	3.5121	2.7117	0.0270
37.885	2.9214	2.2432	0.0126
41.615	2.4940	1.9052	0.0352
	0.06% EtOH-t-butanol		
16.865	9.2429	7.3019	0.02604
18.78	8.1395	6.4138	0.0154
20.60	7.2454	5.6954	0.00088
22.50	6.4450	5.0533	0.01420
24.535	5.7177	4.4708	0.01511
25.52	5.3978	4.2151	0.008359
28.785	4.5275	3.5199	0.0120
32.785	3.6961	2.8579	0.0425
36.835	3.0630	2.3553	0.02240
40.855	2.5750	1.9691	0.0391
	0.6% EtOH-t-butanol		
36.04	3.1554	2.4291	0.03528
41.09	2.5533	1.95193	
46.105	2.10	1.5943	
23.96	5.7251	4.4801	
22.48	6.2178	4.8753	
21.04	6.7545	5.3063	
19.73	7.2986	5.7439	
17.72	8.2097	6.4829	
	1% EtOH-t-butanol		
25.845	5.2181	4.07297	0.02282
29.85	4.2291	3.2832	0.01858
33.855	3.4794	2.6865	0.0127
37.875	2.9137	2.2373	0.02789

Table B.1 (continued)

Average temperature (°C)	V (Cst)	μ (CP)	Coefficient of variation (%)
42.90	2.3670	1.8049	0.03661
24.795	5.5395	4.3300	0.037028
22.785	6.2106	4.8677	0.05969
20.77	6.9927	5.4955	0.06273
18.765	7.9132	6.2356	0.032810

INTERNAL DISTRIBUTION

1. J. M. Begovich
2. R. R. Brunson
3-7. C. H. Byers
8. P. W. Fisher
9. J. R. Hightower
10. F. R. Mynatt
11. D. R. Reichle
12. T. C. Scott
13. C. D. Scott
14. J. S. Watson
15. R. M. Wham
16. J. H. Wilson
17. R. G. Wymer
18. Central Research Library
19. Y-12 Technical Library, Document Reference Section
20-21. Laboratory Records
22. Laboratory Records, R. C.
23. ORNL Patent Section

EXTERNAL DISTRIBUTION

24-28. J. A. Hughes, 5 Lawrence Place, Plymouth Meeting, PA 19462

29. I. L. Thomas, Office of Basic Energy Sciences, DOE, Mail Station J-321, GTN, Washington, DC 20545

30. D. F. Williams, Department of Chemical Engineering, University of Washington, Seattle, WA 98105

31. Office of Assistant Manager for Energy Research and Development, U.S. Department of Energy — ORO, Oak Ridge, TN 37831

32-61. Technical Information Center, Oak Ridge, TN 37830